Chapter 2
Preparation and Characterization of Hybrid Membranes Based on Poly(Ether-*b*-Amide)

Héctor Iván Meléndez-Ortiz, Griselda Castruita-de León, Yibran Perera-Mercado, Jesús Alfonso Mercado-Silva, Bertha Puente-Urbina, Sandra García-Rodríguez, and Luis Alfonso García-Cerda

2.1 Introduction

In the recent decades, there has been an increased interest in developing materials for achieving the separation of certain gases of industrial interest such as carbon dioxide (CO_2) and hydrogen sulfide (H_2S) from natural gas (CH_4) or oxygen (O_2) from nitrogen (N_2). Polymer membranes play an important role in gas separation because of their advantages such as low energy costs, environmental friendliness, and simplicity compared to conventional methods such as aqueous amine scrubbing, cryogenic distillation, or pressure swing adsorption [1–4]. However, a major drawback of polymer-based membranes has been the naturally counteracting permeability and selectivity. It means that the membranes with high permeability usually present a low selectivity and vice versa. Therefore, the development of new membrane materials with improved permeability, selectivity, and stability is required to overcome this drawback and increase the process efficiency for industrial applications.

One strategy for improving membrane selectivity and permeability involves the introduction of inorganic materials into the polymer matrix [5–7]. A variety of inorganic fillers have been explored such as zeolites, carbon molecular sieves, mesoporous silica, metal oxide, carbon nanotubes, metal organic frameworks, and, more recently, graphene [8]. The resulting materials, also called mixed matrix membranes (MMMs), have the advantage of combining the benefits of both phases: thermal resistance of inorganic fillers with the desirable mechanical properties, low price, and good processability of polymers. The inorganic fillers which are dispersed in

H.I. Meléndez-Ortiz (✉) • G. Castruita-de León
CONACyT-Centro de Investigación en Química Aplicada, Blvd. Enrique Reyna Hermosillo 140, Saltillo 25294, Coahuila, México
e-mail: hector.melendez@ciqa.edu.mx

Y. Perera-Mercado • J.A. Mercado-Silva • B. Puente-Urbina
S. García-Rodríguez • L.A. García-Cerda
Centro de Investigación en Química Aplicada, Blvd. Enrique Reyna Hermosillo 140, Saltillo 25294, Coahuila, México

A. Maciel-Cerda (ed.), *Membranes*, DOI 10.1007/978-3-319-45315-6_2

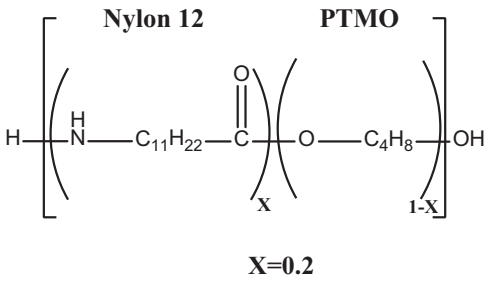

Fig. 2.1 Chemical structure of poly(ether-*b*-amide) (PEBAX® 2533)

polymer matrix change the membrane properties, allowing improved separation performance, compared to unfilled polymer membrane.

The aim of this work is the preparation of MMMs based on poly(ether-*b*-amide) (PEBA) copolymer and mesoporous silica MCM-48 previously modified with 3-aminopropyltrimethoxysilane (APS). PEBA copolymer, best known under the trademark PEBAX®, is a relatively new family of thermoplastic elastomers with unique physical and processing properties. The unique nature of these materials has been attributed to the combination of linear chains of rigid polyamide segments interspaced with flexible polyether segments [9–11]. The high polarity difference between hard and soft segments and the development of a three-dimensional hydrogen-bonding network between the amide units lead to a microphase separated morphology [12]. Membranes made from PEBA copolymers exhibit good permselectivity as well as excellent chemical separation and pervaporation applications because the hard phase provides high selectivity and mechanical strength and the soft one offers high permeability due to the great chain mobility of the ether linkage (Fig. 2.1) [13].

On the other hand, MCM-48 silica is found to be attractive for potential application in membranes for gas separation due to its three-dimensional interconnected cubic pore structure which is less prone to pore blocking than the unidimensional hexagonal arrangement in MCM-41 silica. Also, mesoporous silica MCM-48 shows fascinating properties as tunable pore sizes, uniform mesopores, and high surface area. There are some reports about the preparation of MMMs based on PEBA copolymers and some fillers such as silica [14, 15], zeolites [16, 17], multiwalled carbon nanotubes [18, 19], and polyoctahedral oligomeric silsesquioxanes [20]. However, as far as we know, there is no report about the preparation of MMMs of PEBA with amine-modified MCM-48 silica. The modification of MCM-48 with compounds containing amine groups could be useful for either to improve the filler–polymer interface compatibility or to facilitate the transport of CO_2 [15, 21, 22]. The motivation of this work is to gain insight into the effect of incorporation of amine-modified MCM-48 upon the thermal properties, morphology, as well as gas separation performance of the prepared hybrid membranes. MMMs of PEBA and APS-modified MCM-48 silica were successfully prepared using the methodology reported in this work. The previous modification of MCM-48 with the amine organosilane improved the interaction with the PEBA matrix. The gas separation performance of pristine PEBA membranes was improved with the addition of the inorganic material.

2.2 Experimental Section

2.2.1 Materials

Poly(ether-*b*-amide) (PEBAX® 2533) in pellet form was obtained from Arkema, and chloroform 99 % (CH_3Cl) from J. T. Baker was used in the preparation of MMMs. Tetraethylorthosilicate 98 %, TEOS, and cetyltrimethylammonium bromide 98 %, CTAB, were supplied from Aldrich. Deionized water was obtained from a system of two ionic interchange columns in a Cole-Parmer Instrument. Ethanol 99 % from J. T. Baker and aqueous ammonia solution 29 %, NH_4OH, from Fermont were used to prepare mesoporous MCM-48 materials. In addition, 3-aminopropyltrimethoxysilane (APS) 97 %, APS, (Aldrich), isopropanol 99 % (Aldrich), and toluene 99 % (J. T. Baker) were used to modify the mesoporous MCM-48 silica.

2.2.2 Synthesis and Functionalization of MCM-48 Mesoporous Silica

MCM-48 was synthesized and functionalized as previously reported by our research group [23]. Briefly, 6.8 g of TEOS was added to a solution containing 5.2 g of CTAB, 240 g of H_2O, 100 mL of ethanol, and 24 mL of NH_4OH. Then, the solid product was dried at room temperature and further calcined at 540 °C. The modification of the calcined MCM-48 silica was carried out by adding the silica material to a mixture containing APS and toluene. The reaction mixture was vigorously stirred under reflux for 15 h and then the solid was washed with isopropanol.

2.2.3 Preparation of the APS-MCM-48/PEBA Membranes

Flat PEBA and APS-MCM-48/PEBA membranes were prepared to evaluate its gas separation performance. To prepare the pristine PEBA membranes, polymeric pellets were dissolved at 35 °C in chloroform (10 wt%) to obtain an appropriate viscosity for casting the solution. To prepare MMMs based on PEBA and APS-MCM-48, some parameters were evaluated in order to obtain membranes for gas separation studies. The parameters evaluated were the amount of modified silica, solution viscosity, sonication, and stirring time. Thus, MMMs were fabricated as follows: APS-MCM-48 silica (2.5–10 wt% with respect to the total content of PEBA) was dispersed in 1 mL of $CHCl_3$ containing a small amount of PEBA (0.02 g) by using an ultrasonic processor for 5 min and then sonicated in an ultrasonic bath for 10 min. After that, 3 mL of a PEBA solution (10 wt% polymer in $CHCl_3$) was added under vigorous stirring to the solution containing dispersed APS-MCM-48 silica, and the resulting solution was magnetically stirred at 35 °C for 24 h. It is worthy to mention

that no evaporation of $CHCl_3$ was observed during the preparation of polymer solutions. Before the membrane casting, three intervals of sonication of 15 min were carried out to ensure a well-dispersed solution. Subsequently, the homogeneous solution was poured on a plain glass surface and left overnight covered with a glass cover at room temperature for natural and slow evaporation. After that, MMMs were heated at reduced pressure to remove the solvent remaining within the membrane. The treatment took place in a vacuum oven at intervals of temperature of 10 °C from 30 to 60 °C for 8 h each. Membrane thicknesses were measured by a Digimatic Micrometer 0–30 mm (accuracy ± 1 mm).

2.2.4 Characterization

MCM-48 silica was characterized by X-ray diffraction (XRD) using a SIEMENS D5000 diffractometer with CuKα radiation. The diffraction data were recorded in the 2θ range of 2–10°. Nitrogen adsorption–desorption isotherm was obtained on Quantachrome AS1Win equipment at −196 °C. Before the experiments, the mesoporous material was degassed under vacuum at 120 °C. The specific surface area of the sample was calculated using a Brunauer–Emmett–Teller (BET) method, and the pore size distribution was calculated using desorption branches of nitrogen isotherms and a method according to Density Functional Theory (DFT). Transmission electron microscopy (TEM) was performed using an HRTEM Titan operated at 300 kV. MMMs were characterized by Fourier transform infrared spectroscopy (FT-IR) by using a Nicolet Magna 550 spectrophotometer, equipped with a Universal ATR sampling accessory. TGA studies were carried out using a TGA Q500 apparatus (TA Instruments, New Castle, DE) under nitrogen flow. The morphology of MMMs was examined using a scanning electron microscope JEOL JSM-7401F.

2.2.5 Permeability Measurements

Gas permeability coefficients for three pure gases, methane (CH_4), carbon dioxide (CO_2), and nitrogen (N_2), were measured at 35 °C and 2 atm using a variable pressure permeation cell. The permeability (P, Barrer, and 1 Barrer = 10^{-10} cm^3 (STP) cm/(cm^2 s cmHg)) was determined by the time-lag method under steady-state conditions according to the next equation:

$$P = \frac{V l R^N}{ART}\left[\frac{\left(\mathrm{d}p/\mathrm{d}t\right)}{\Delta p}\right] \tag{2.1}$$

where V is the inferior volume of the permeation cell (cm^3), l is the membrane thickness (cm), T is the temperature (K), A is the effective membrane area (cm^2), Δp is the

pressure of the superior volume of permeation cell (mmHg), *dp*/*dt* is the increase of the pressure with respect to time (mmHg s^{-1}), R^N is the molar volume of gas at constant temperature and pressure (22,415 cm^3 (STP) cmHg mol^{-1} K^{-1}), and *R* is the universal constant of gases (62,634 cm^3 (STP) cmHg mol^{-1} K^{-1}). Ideal gas separation factors (α) were calculated from the ratio of pure gas permeability coefficients using the following equation:

$$\alpha_{A/B} = P_A / P_B \tag{2.2}$$

where P_A and P_B are gas permeability coefficients of the pure gases A and B, respectively.

2.3 Results and Discussion

2.3.1 Characterization of Amine-Modified MCM-48 Silica

The powder XRD patterns of the pristine and amine-modified mesoporous silica MCM-48 are shown in Fig. 2.2a. The XRD diffractogram for bare MCM-48 silica displayed reflection peaks at 2θ values of 2.7 (211) and 3.1 (220) and signals between 4.5 and 5.8 corresponding to the planes (321), (400), (420), (332), (422), and (431) which are characteristics for this silica. After modification with APS, the XRD patterns of MCM-48 did not show significant changes which indicated that the structure of MCM-48 was preserved after modification. However, the peaks between 4.5 and 5.8 disappeared. This behavior indicated the pore filling of MCM-48 silica by APS but not changes in the mesostructure [24]. The FT-IR spectra of pristine and amine-modified MCM-48 are shown in Fig. 2.2b. MCM-48 silica exhibited a signal at 3741 cm^{-1} assigned to the O–H bond of the silanol groups, a band at 1058 cm^{-1} due to Si–O–Si stretching vibration, and a peak at 800 cm^{-1} corresponding to the bending vibration for the bond Si–O–Si. On the other hand, the FT-IR spectrum of APS-MCM-48 showed a signal at 1560 cm^{-1} assigned to the NH_2 scissor from APS [25]. Also, it can be seen that the band of Si–O–H (3740 cm^{-1}) disappeared in the spectrum of APS-MCM-48 which evidences the covalent grafting of APS on MCM-48 silica. Figure 2.2c shows the pore size distribution of MCM-48 and APS-MCM-48. The average pore size was estimated to be 2.2 and 1.5 nm for MCM-48 and APS-MCM-48, respectively. After modification, the surface area and pore volume decreased from 1912 to 450 m^2/g and from 0.876 to 0.245 m^3/g, respectively, due to the pore filling effect of APS. Thermogravimetric analysis (TGA) was used to determine the amount of APS grafted onto the inorganic material (Fig. 2.2d). Unmodified MCM-48 silica was stable in the temperature range from 30 to 750 °C, while APS-MCM-48 showed a weight loss of 3 % before 100 °C due to desorption of moisture. Also, it was observed a small weight loss between 110 and 170 °C probably due to the loss of NH_3 from APS and then a main weight loss in the temperature range of 200–600 °C due to chemical decomposition of the grafted APS.

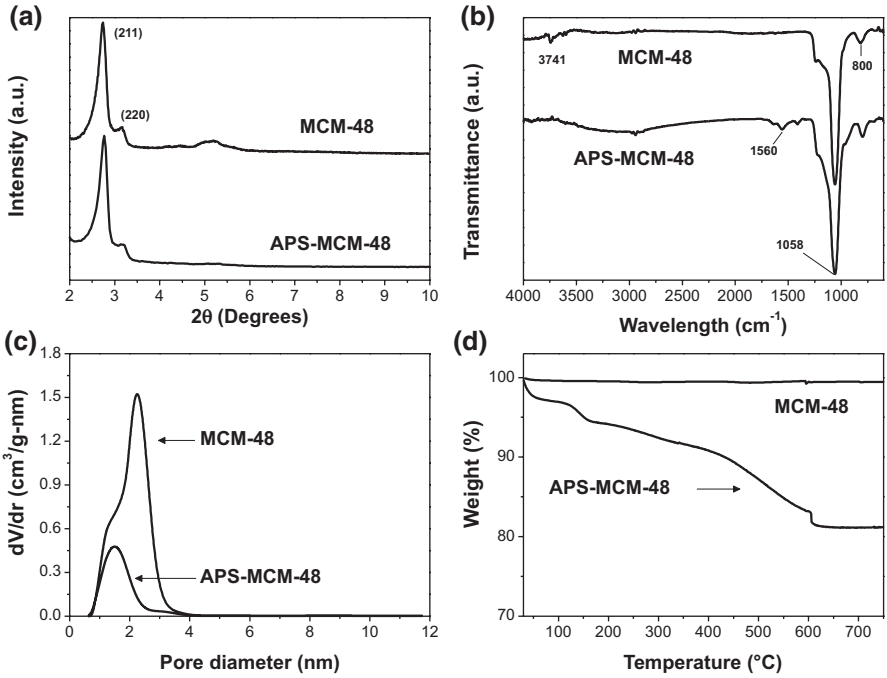

Fig. 2.2 Characterization of unmodified and modified MCM-48 silica: (**a**) X-ray powder diffraction pattern, (**b**) FT-IR spectroscopy, (**c**) particle size distribution, and (**d**) thermogravimetric study

2.3.2 MMMs Characterization

2.3.2.1 FT-IR Spectroscopy

PEBA copolymer consists of both flexible poly(tetramethylene oxide) (PTMO) segments and rigid polyamide segments (nylon 12). The FT-IR spectrum of pristine PEBA showed signals at 3295 and 1645 cm^{-1} due to the stretching vibrations of the N–H bond and the C = O bond from polyamide segment, respectively (Fig. 2.3). The strong bands at 2935 and 2859 cm^{-1} correspond to the stretching vibration of the C–H bond from methylene groups. In addition, the peaks at 1733 and 1108 cm^{-1} represent the O–C = O and C–O–C stretching vibrations, respectively. The FT-IR spectrum obtained for APS-MCM-48/PEBA hybrid membrane is very similar to that for the pristine PEBA copolymer. However, it can be observed a weak band at 1160 cm^{-1} probably due to the Si–O–Si from MCM-48 silica.

2.3.2.2 SEM Studies

The morphology of the prepared membranes was investigated using scanning electron microscopy (SEM). The cross-sectional SEM images of pristine PEBA and APS-MCM-48/PEBA membranes at different amounts of amine-modified filler are

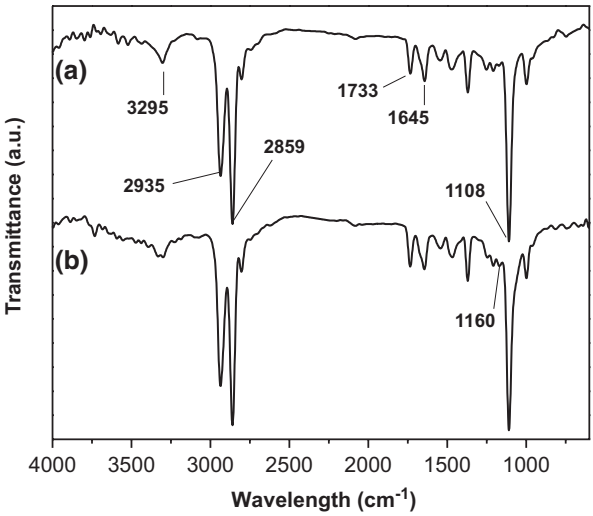

Fig. 2.3 FT-IR spectra for: (**a**) pristine PEBA membrane and (**b**) APS-MCM-48 (10 %)/ PEBA membrane

shown in Fig. 2.4. Pristine PEBA membrane showed a smooth morphology free of voids with some small roughness areas. On the other hand, the SEM images for hybrid membranes showed that the spherical APS-functionalized MCM-48 silica particles were uniformly dispersed throughout PEBA matrix in a concentration range of 2.5–10 wt%. The APS-functionalized MCM-48 particles were completely surrounded by polymer matrix and no voids were formed, as shown in Fig. 2.4b–e, suggesting that the grafted APS on the external surface of MCM-48 silica enhanced the filler–polymer interface compatibility.

2.3.2.3 Thermal Properties

The study of the thermal properties, especially the stability and decomposition processes of the membrane materials, is important for understanding and eventually improving their gas separation performance. TGA of pristine PEBA membrane showed that there was no weight loss up to 350 °C indicating that the solvent was removed with the treatment at 60 °C (Fig. 2.5). Above this temperature, the PEBA copolymer starts to dramatically decompose until 470 °C due to the main chain scission. Similar behavior was observed for APS-MCM-48/PEBA membranes at different contents of modified silica. However, a slight decrease in the thermal stability was observed, and it was more evident when the content of silica was increased. This could be related to a disruption caused by the silica particles in the rigid polyamide domains. The remaining weight loss allowed the verification of the nominal wt% loading of the amine-modified MCM-48 present in the corresponding MMM, i.e., 0, 4.7, and 9.0 wt% residual contents for nominal 0, 5, and 10 wt%, respectively.

DSC studies were carried out in a temperature range of 20–250 °C. The DSC thermograms of pristine PEBA and hybrid PEBA membranes with different contents of APS-MCM-48 are shown in Fig. 2.6. The DSC thermogram of pristine

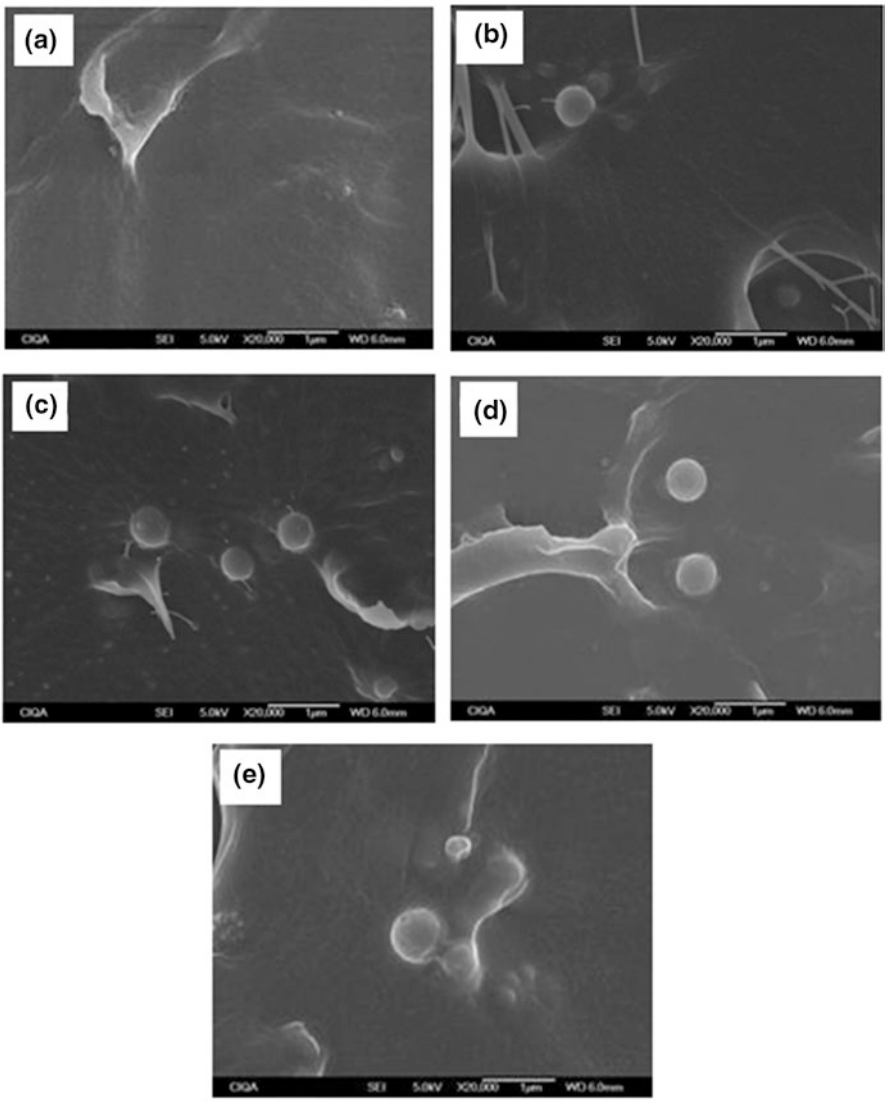

Fig. 2.4 Cross-sectional SEM images for (**a**) pristine PEBA membrane and MMMs with different contents of APS-MCM-48: (**b**) 2.5 %, (**c**) 5 %, (**d**) 7.5 %, and (**e**) 10 %. Magnification × 20,000

PEBA only showed one endothermic transition at 139 °C. This transition is due to the melting of the polyamide domains [9, 20]. Even after the incorporation of APS-MCM-48, this peak transition was visible, and its shape remained unchanged. However, a slight decrease of this transition to lower temperature was observed with increasing filler loading. This may be due to a disruption caused by the silica particles in the rigid polyamide domains as it was observed in TGA results.

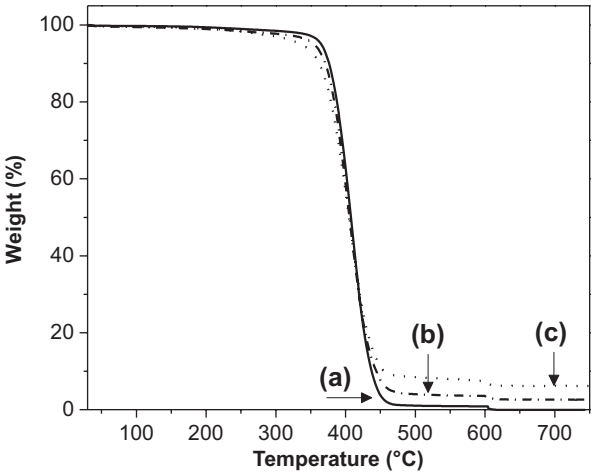

Fig. 2.5 Thermogravimetric curves for (**a**) pristine PEBA and hybrid membranes with contents of APS-MCM-48 of (**b**) 5 and (**c**) 10 wt%

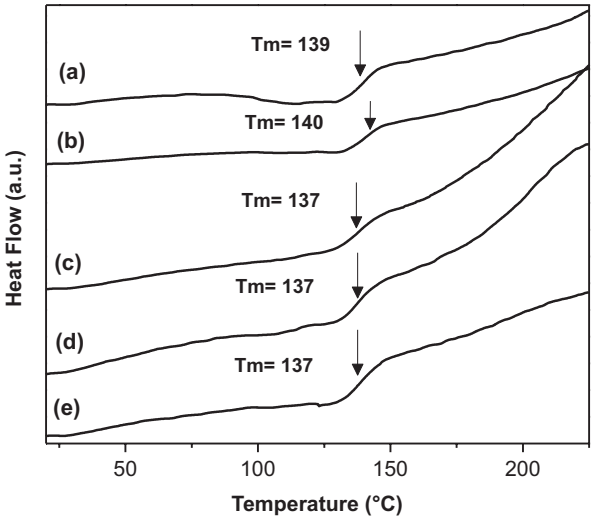

Fig. 2.6 DSC thermograms for (**a**) pristine PEBA and hybrid membranes with different contents of APS-MCM-48 of (**b**) 2.5, (**c**) 5, (**d**) 7.5, and (**e**) 10 wt%

2.3.2.4 Pure Gas Permeation Performance

The permeation performance of the pristine PEBA and hybrid membranes with filler contents of 2.5 and 5 wt% was tested using pure gas (CH_4, CO_2, and N_2) under dry state. Permeability and ideal selectivity values for the selected membranes are shown in Table 2.1. Pristine PEBA membranes showed high values of permeability for CO_2 which agrees with those reported previously [15, 20]. This behavior was attributed to the strong affinity between the PTMO units and CO_2 molecules. On the other hand, a decrease in permeability values was found for the hybrid membranes. The CO_2 permeability decreased from 470 Barrer for pristine PEBA membrane to 347 Barrer for the APS-MCM-48/PEBA membrane with 5 wt% loading. However,

Table 2.1 Pure gas permeability and ideal selectivity of the PEBA and hybrid membranes at 2 atm of pressure and 35 °C

	Permeability (Barrer)			Selectivity	
Membrane	CO_2	CH_4	N_2	CO_2/CH_4	CO_2/N_2
PEBA	470.82	97.51	31.80	4.82	14.80
MCM-48-APS (2.5 %)/PEBA	364.90	59.39	19.54	6.14	18.67
MCM-48-APS (5 %)/PEBA	347.87	81.78	28.37	4.25	12.26

in comparison with pristine PEBA membranes, MMM with 2.5 % of APS-MCM-48 exhibited higher ideal CO_2/CH_4 and CO_2/N_2 ideal selectivity, and the increment of CO_2/N_2 selectivity was higher than CO_2/CH_4 selectivity. The higher selectivity of MMMs may be due to the presence of amine groups which may effectively enhance the adsorbent affinity toward CO_2 [22, 26]. The amine groups in the pore channels and on the surface of MCM-48 tended to adsorb more CO_2 molecules, making a contribution to the increase of selectivity.

2.4 Conclusions

Mixed matrix membranes were prepared by incorporating amine-modified MCM-48 into the PEBA matrix. The modification of MCM-48 with APS not only improved the filler–polymer interface compatibility but also permitted an appropriated dispersion of the spherical APS-MCM-48 nanoparticles. The incorporation of APS-MCM-48 modified slightly the thermal properties of the pristine PEBA membrane. APS-MCM-48 (2.5 %)/PEBA membrane showed an improvement in CO_2/CH_4 and CO_2/N_2 selectivity. Hence, it can be concluded that APS-MCM-48 may be a suitable nanofiller to improve the gas separation performance of PEBA copolymer membranes.

Acknowledgments This work was funded by CONACYT-México (Fondo SENER-Hidrocarburos) under Grant No. 127499. Authors H. I. Melendez-Ortiz and G. Castruita-de Leon are grateful to the program Catedras-CONACyT. The authors are grateful to J. A. Cepeda, G. Mendez, and J. Sanchez for their technical assistance in the SEM, TGA, and FT-IR studies, respectively.

References

1. Xing, R., & Ho, W. S. W. (2011). Crosslinked polyvinylalcohol–polysiloxane/fumed silica mixed matrix membranes containing amines for CO_2/H_2 separation. *Journal of Membrane Science, 367*, 91–102.
2. Yang, H. Q., Xu, Z. H., Fan, M. H., Gupta, R., Slimane, R. B., Bland, A. E., et al. (2008). Progress in carbon dioxide separation and capture: A review. *Journal of Environmental Sciences, 20*, 14.
3. Ge, L., Zhu, Z., & Rudolph, V. (2011). Enhanced gas permeability by fabricating functionalized multi-walled carbon nanotubes and polyethersulfone nanocomposite membrane. *Separation and Purification Technology, 78*, 76.

4. Sanipa, S. M., Ismail, A. F., Goh, P. S., Soga, T., Tanemura, M., & Yasuhiko, H. (2011). Gas separation properties of functionalized carbon nanotubes mixed matrix membranes. *Separation and Purification Technology, 78*, 208.
5. Chung, T. S., Jiang, L. Y., Li, Y., & Kulprathipanja, S. (2007). Mixed matrix membranes (MMMs) comprising organic polymers with dispersed inorganic fillers for gas separation. *Progress in Polymer Science, 32*, 483.
6. Rafiq, S., Mana, Z., Maulud, A., Muhammada, N., & Maitra, S. (2012). Separation of CO_2 from CH_4 using polysulfone/polyimide silica nanocomposite membranes. *Separation and Purification Technology, 90*, 162.
7. Mahajan, R., Burns, R., Schaeffer, M., & Koros, W. J. (2002). Challenges in forming successful mixed matrix membranes with rigid polymeric materials. *Journal of Applied Polymer Science, 86*, 881.
8. Goh, P. S., Ismail, A. F., Sanip, S. M., Ng, B. C., & Aziz, M. (2011). Recent advances of inorganic fillers in mixed matrix membrane for gas separation. *Separation and Purification Technology, 81*, 243.
9. Armstrong, S., Freeman, B., Hiltner, A., & Baer, E. (2012). Gas permeability of melt-processed poly(ether block amide) copolymers and the effects of orientation. *Polymer, 53*, 1383.
10. Chen, J. C., Feng, X., & Penlidis, A. (2004). Gas permeation through poly(Ether-*b*-amide) (PEBAX 2533) block copolymer membranes. *Separation Science and Technology, 39*, 149.
11. Tocci, E., Gugliuzza, A., De Lorenzo, L., Macchionea, M., De Luca, G., & Drioli, E. (2008). Transport properties of a co-poly(amide-12-b-ethylene oxide) membrane: A comparative study between experimental and molecular modelling results. *Journal of Membrane Science, 323*, 316.
12. Peyravi, M., Babaluo, A. A., Ardestani, M. A., Razavi Aghjeh, M. K., Pishghadam, S. R., & Hadi, P. (2010). Study on the synthesis of poly(ether-block-amide) copolymer based on nylon6 and poly(ethylene oxide) with various block lengths. *Journal of Applied Polymer Science, 118*, 1211.
13. Ardestani, M. A., Babaluo, A. A., Peyravi, M., Razavi Aghjeh, M. K., & Jannatdoost, E. (2010). Fabrication of PEBA/ceramic nanocomposite membranes in gas sweetening. *Desalination, 250*, 1140.
14. Tan, H. F., Wu, Y. H., Zhou, Y., Liu, Z. N., & Li, T. M. (2014). Pervaporative recovery of n-butanol from aqueous solutions MCM-41 filled PEBA mixed matrix membrane. *Journal of Membrane Science, 453*, 302.
15. Wu, H., Li, X., Li, Y., Wang, S., Guo, R., Jiang, Z., et al. (2014). Facilitated transport mixed matrix membranes incorporated with amine functionalized MCM-41 for enhanced gas separation properties. *Journal of Membrane Science, 465*, 78.
16. Friess, K., Hynek, V., Šípek, M., Kujawski, W. M., Vopicka, O., Zgazar, M., et al. (2011). Permeation and sorption properties of poly(ether-block-amide) membranes filled by two types of zeolites. *Separation and Purification Technology, 80*, 418.
17. Murali, R. S., Ismail, A. F., Rahman, M. A., & Sridhar, S. (2014). Mixed matrix membranes of Pebax-1657 loaded with 4A zeolite for gaseous separations. *Separation and Purification Technology, 129*, 1.
18. Murali, R. S., Sridhar, S., Sankarshana, T., & Ravikumar, Y. V. L. (2010). Gas permeation behavior of Pebax-1657 nanocomposite membrane incorporated with multiwalled carbon nanotubes. *Industrial and Engineering Chemistry Research, 49*, 6530.
19. Hong-Wei, Y., Chen, Z. H., & Yang, I. K. (2012). Use of the composite membrane of poly(ether-block-amide) and carbon nanotubes (CNTs) in a pervaporation system incorporated with fermentation for butanol production by Clostridium acetobutylicum. *Bioresource Technology, 109*, 105.
20. Rahman, M. M., Filiz, V., Shishatskiy, S., Abetz, C., Neumann, S., Bolmer, S., et al. (2013). PEBAX® with PEG functionalized POSS as nanocomposite membranes for CO_2 separation. *Journal of Membrane Science, 437*, 286.

21. Khan, A. L., Klaysom, C., Gahlaut, A., & Vankelecom, I. F. J. (2013). Polysulfone acrylate membranes containing functionalized mesoporous MCM-41 for CO_2 separation. *Journal of Membrane Science, 436*, 145.
22. Kim, S., & Marand, E. (2008). High permeability nano-composite membranes based on mesoporous MCM-4 nanoparticles in a polysulfone matrix. *Microporous and Mesoporous Materials, 114*, 129.
23. Meléndez-Ortiz, H. I., Perera-Mercado, Y., Mercado-Silva, J. A., Olivares-Maldonado, Y., Castruita, G., & García-Cerda, L. A. (2014). Functionalization with amine-containing organosilane of mesoporous silica MCM-41 and MCM-48 obtained at room temperature. *Ceramics International, 40*, 9701.
24. Mercier, L., & Pinnavaia, T. J. (1998). Heavy metal ion adsorbents formed by the grafting of a thiol functionality to mesoporous silica molecular sieves: Factors affecting Hg (II) uptake. *Environmental Science and Technology, 32*, 2749.
25. Yokoi, T., Yoshitake, H., & Tatsumi, T. (2004). Synthesis of amino-functionalized MCM-41 via direct co-condensation and post-synthesis grafting methods using mono-, di-and tri-amino-organoalkoxysilanes. *Journal of Materials Chemistry, 14*, 951.
26. Yue, M. B., Chun, Y., Cao, Y., Dong, X., & Zhu, J. H. (2006). CO_2 capture by as-prepared SBA-15 with an occluded organic template. *Advanced Functional Materials, 16*, 1717.

http://www.springer.com/978-3-319-45314-9

Membranes
Materials, Simulations, and Applications
Maciel-Cerda, A. (Ed.)
2017, XIII, 154 p. 92 illus., 48 illus. in color., Hardcover
ISBN: 978-3-319-45314-9